Microporous and Mesoporous Materials 117 (2009) 170–177

Contents lists available at ScienceDirect

Microporous and Mesoporous Materials

journal homepage: www.elsevier.com/locate/micromeso

Incorporation of Pd nanoparticles in mesostructured silica

J. Garcia-Martinez [a,*], N. Linares [a], S. Sinibaldi [a], E. Coronado [b], A. Ribera [b,*]

[a] Departamento de Química Inorgánica, Universidad de Alicante, Carretera San Vicente s/n, E-03690 Alicate, Spain
[b] Instituto de Ciencia Molecular, Universidad de Valencia, Edificios Institutos de Paterna, Polígono la Coma s/n, E-46980 Paterna, Spain

ARTICLE INFO

Article history:
Received 17 February 2007
Received in revised form 16 June 2008
Accepted 19 June 2008
Available online 9 July 2008

Keywords:
MCM-41
Pd
Nanoparticles
Mesoporous
Catalysis

ABSTRACT

Monodisperse Pd nanoparticles were prepared by controlled reduction in organic phase and subsequent transfer to aqueous phase. A systematic study was carried out to finely tune nanoparticle size and optimize particle size distribution. The use of 4-dimethylaminopyridine as a transfer agent allowed for the easy and quantitative extraction of the Pd to the aqueous phase. The quaternary amine-functionalized metal nanoparticles were then used as metallic micelle replicas to grow silica around them. This novel and facile metal incorporation method provided an excellent dispersion and homogeneity of Pd nanoparticles on silica supports. In addition, cationic surfactants, such as cetyltrimethylammonium bromide, can be used to produce mesoporosity in these nanoparticles-containing silicas. As an alternative, the metal nanoparticles were functionalized with alkoxysilanes by covalent binding using mercaptopropyltriethoxysilane and then co-polymerized with tetraethoxysilane *via* basic-catalyzed hydrolysis in the presence of cationic surfactants.

1. Introduction

The preparation and processing of metal nanoparticles is a field of current interest in materials chemistry because of the possibility to induce emerging physical (magnetic, electrical or optical) or chemical (catalytic) properties when particle size reaches the nanometer range [1–5]. More specifically, metals used in catalysis are nanoparticles rather than large single crystals, because of their higher dispersion (fraction of atoms in the surface shell), higher number of defects – which provides favourable bonding opportunities for breaking and forming bonds –, easier surface reconstruction to adapt to the adsorbates, better interaction with the support, and tunable electronic properties varying particle size [1]. Current goals regarding the preparation of nanoparticles are: higher particle size monodispersity and smaller average size, in the range where most pronounced size-dependent properties emerge. In this context, sols produced in organic media (organosols), such as toluene, have been widely used as these produce highly monodisperse nanoparticles that can be then readily transferred to aqueous media if desired.

Metal nanoparticles, however, tend to agglomerate to reduce their surface tension and are difficult to recover because of its small size. To avoid these drawbacks, metal nanoparticles are typically loaded on porous supports, what prevents agglomeration and make their handling and recovery easier [1]. Although supports are typically inert (silica, alumina, carbon, etc.) in some cases, some surface chemistry (such as acidicity, basicity or redox properties) is introduced to further tune the catalytic activity of the nanoparticles *via* metal-support interaction. Also, the porosity of the support can be developed in a manner that the nanoparticles loading is more homogenous and agglomeration greatly reduced. In the last decade, mesostructured supports with controlled and uniform porosity have been prepared by surfactants-assisted self-assembly. Especially relevant is the case of ordered mesoporous silica materials, such as MCM-41 and related materials, firstly reported in the early 90′s [6]. Since then, numerous articles have been devoted to their use as a catalysts supports [7–14]. A wide range of metal nanoparticles have been loaded on these mesoporous materials [15–23] by different techniques, such as ion-exchange, chemical grafting, chemical vapor deposition and impregnation including incipient wetness impregnation [24–38]. In some cases, either the decomposition or the reduction of the metal precursor is required. All these techniques have in common that the metal is loaded on a pre-existing support. This may cause an inhomogeneous loading, especially if the size of the nanoparticles is similar or larger than the pore size of the support. In this case, the nanoparticles are mainly located on the external surface of the support causing poor metal dispersion. Even if the nanoparticles are homogeneously loaded on the pores, they can agglomerate and leach under reaction conditions. As an alternative, metal nanoparticles can be, at least partially, incorporated in the support internal structure, by embedding them in the pore walls. This strategy significantly reduce both agglomeration and leaching, still providing enough accessibility to the reactants

* Corresponding authors.
E-mail address: j.garcia@ua.es (J. Garcia-Martinez).

1387-1811/$ - see front matter © 2008 Elsevier Inc. All rights reserved.
doi:10.1016/j.micromeso.2008.06.038

(nanoparticle size being larger than pore wall thickness). Using a different strategy, Chytil et al. [39] have encapsulated Pt nanoparticles (6–10 nm) capped with EG-PGEG copolymer in mesoporous silica SBA-15 (0.1 wt.% Pt). The encapsulated nanoparticles maintained their original size, however some of their surface was not accessible by hydrogen chemisorption or during toluene hydrogenation.

In 2005, Aprile et al. [40] develop a new strategy to incorporate gold nanoparticles in a mesoporous material using *N*-[3-(triethoxysilyl)propyl] O-2-(dicetylmethylammonium)ethyl urethane as a ligand stabilizer. This molecule which interacts with gold nanoparticles through the quaternary ammonium ions undergoes co-condensation with tetraethoxysilane during the formation of the silica through the terminal triethoxysilyl groups. Later on, the same molecule has been used to functionalize the magnetite nanoparticles by covalent bonding with condensation with the triethoxysilyl terminal groups [41]. The quaternary dicetyl ammonium group is then used as a mesopore forming agent employing the same experimental conditions typically used in the preparation of MCM-41-type silicas. Recently, Budroni and co-workers have prepared a new material in which Pd nanoparticles capped with 1-dodecanethiol and 3-mercaptopropyltrimethoxysilane have been incorporated to a sponge-like porous silica [42,43].

Herein, we describe a simple and versatile method to incorporate metal nanoparticles in porous materials by using metal nanoparticles conveniently functionalized as templating agents for mesoporous silica formation. This strategy has been used both by (i) functionalizing the metal nanoparticles with cationic groups to induce the formation of silica around them by a M^+I^- mechanism, similar to the one proposed for the synthesis of mesostructured materials with cationic surfactants, namely S^+I^-, or by (ii) functionalizing the metal nanoparticles with a thiol-terminal triethoxysilane and subsequent co-polymerization with a silica precursor, typically tetraethoxysilane, during the support formation. Both methods can be carried out in the presence of surfactants, such as cetyltrimethylammonium bromide, to induce the formation of controlled and uniform mesoporosity.

2. Experimental

2.1. Synthesis of the Pd nanoparticles

Pd nanoparticles, were obtained by reduction of $[PdCl_4]^{2-}$ with $NaBH_4$ and subsequent stabilization using tetraoctylammonium bromide ($(N(C_8H_{17})_4)Br$) as a capping agent. The method is a variation of that proposed by Brust et al. [44]. In a typical synthesis, 15 mL of a 30 mM aqueous solution of Na_2PdCl_4 (yellow color) was mixed with 40 mL of a 50 mM solution of tetraoctylammonium bromide in toluene. Two hours later, the complete transfer of the $[PdCl_4]^{2-}$ from the aqueous solution to the organic phase was observed, as evidenced by the red–brown color in the organic phase due to the $[PdCl_4]^{2-}$ anion. The colorless water phase was eliminated and the toluene phase dried with Na_2SO_4. Then, 11.4 mL of a freshly prepared 0.1 M $NaBH_4$ aqueous solution was slowly added under vigorous stirring. The mixture was stirred overnight, washed with 40 mL of a 0.1 M H_2SO_4 aqueous solution, 40 mL of a 0.1 M NaOH aqueous solution, and finally three times with 40 mL of water. The organosol was then dried over anhydrous Na_2SO_4. The experimental conditions were systematically varied to optimize the Pd particle size distribution by controlling: (i) the capping agent concentration, (ii) the reducing agent concentration, (iii) the water contained in the $[PdCl_4]^{2-}$/toluene solution and (iv) the rate of stirring during the Pd(II) reduction step (see Table 1).

Table 1
Influence of various synthesis parameter on the particle size of Pd nanoparticles prepared by reduction of $[PdCl_4]^{2-}$ with $NaBH_4$ in toluene

Sample	$[(N(C_8H_{17})_4)Br]$ (mol/L)	$[NaBH_4]$ (mol/L)	Added water to Pd in toluene (μL)	Stirring rate (rpm)	Particle size (nm)
Pd-5	25	0.8	0	800	1.66 ± 0.50
Pd-6	50	0.8	0	800	1.22 ± 0.15
Pd-18	100	0.8	0	800	2.14 ± 0.46
Pd-21	50	0.8	50	800	2.07 ± 0.64
Pd-22	50	0.8	250	800	1.51 ± 0.51
Pd-23	50	0.8	500	800	1.74 ± 0.84
Pd-24	50	0.1	0	800	1.72 ± 0.81
Pd-25	50	0.4	0	800	1.30 ± 0.57
Pd-27	50	1.2	0	800	1.39 ± 0.29
Pd-29	50	0.1	0	400	1.61 ± 0.88
Pd-31	50	0.1	0	1200	1.20 ± 0.55
Pd-32	50	0.1	0	1600	1.03 ± 0.27

2.2. Transfer the Pd nanoparticles to the water phase

This step was performed following the method described by Gittins and Caruso [45]. An aqueous 0.1 M 4-dimethylaminopyridine (DMAP) solution (10 mL), used as a transfer agent, was added to 40 mL of the as-prepared Pd nanoparticles in toluene. The mixture was stirred for 2 h. These conditions were sufficient to complete transfer of the Pd nanoparticles to the aqueous phase. As described elsewhere [45], the equilibrium (neutral/zwitterion) of the DMAP allows for a fast and efficient transfer of the metal from the toluene (neutral DMAP/Pd nanoparticle) to the aqueous phase (zwitterion DMAP/Pd nanoparticle).

2.3. Synthesis of mesoporous silica materials containing Pd nanoparticles

4-Dimethylaminopyridine (DMAP), which served in the previous step to extract the Pd nanoparticles from the toluene to the aqueous phase, was also used as the quaternary ammine polar head of a metallic replica of a surfactant micelle formed by the DMAP and the metallic hydrophobic core. The Pd-nanoparticles-containing silica was obtained by hydrolysis of tetraethylorthosilicate (TEOS) with ammonia in the presence of DMAP-functionalized Pd nanoparticles. Controlled mesoporosity can be also introduced in these nanoparticles-containing silica by the addition of cetyltrimethylammonium bromide (CTAB), commonly used in the synthesis of MCM-41 type materials. The synthesis of this material described by Berenguer-Murcia et al. [46] was judiciously adapted to incorporate Pd nanoparticles in the silica walls. More specifically, in a typical synthesis (see Table 2) 55 mg of CTAB were dissolved in 2.6 mL of deionized water containing 240 μL of the NH_4OH solution by heating the mixture to 50 °C while stirring, until a clear solution was observed. Then 5 mL of the Pd aqueous sol described in the previous section were added. Finally, 290 μL of TEOS were mixed to this suspension. The resulting gel was stirred overnight at room temperature and then hydrothermally treated at 150 °C in a stainless steel Teflon-lined autoclave, under static conditions for 48 h. The solid obtained was washed thoroughly with water and dried at room temperature overnight. The calcinations of these materials were carried out in a nitrogen flow for 4 h at 550 °C and then switch to oxygen for 8 h more.

Alternatively, the Pd nanoparticles were used as silica precursors by functionalization with 3-mercaptopropyltriethoxysilane (MPTES). Their co-polymerization with TEOS by base-catalyzed hydrolysis in the presence of CTAB produced MCM-41 type silica with Pd nanoparticles homogeneously incorporated in its mesopores walls. In a typical synthesis (see Table 2), 55 mg of CTAB were dissolved in 2.6 mL of deionized water containing 240 μL of the

Table 2
Synthesis parameters studied to incorporate DMAP or thiol-functionalized Pd nanoparticles in high quality MCM-41

Experiment	CTAB (mg)	TEOS (μL)	NH_4OH (33 wt.%) (μL)	MPTES (μL)
1	53	150	240	54
2	53	150	240	0
3	53	150	240	27
4	53	150	240	5.4
8	28	150	120	54
9	28	150	120	0
10	28	150	120	27
11	28	150	120	5.4
12	55	290	240	54
13	55	290	240	0
14	55	290	240	27
15	55	290	240	5.4
15dil	55	290	240	0.54

5 mL of Pd sol (4.8 g Pd/L) were mixed in 2.6 mL of water with the following amounts of reactants.

NH_4OH solution by heating the mixture to 50 °C while stirring, until a clear solution was observed (solution A). In parallel, 5.4 μL of MPTES were added to 5 mL of the Pd aqueous sol described in the previous section (solution B). After stirring this solution for 15 min, its color changed from reddish to yellow-brown indicating that most of the Pd nanoparticles were functionalized by the thiol. At that point, the solution A was added to solution B and kept under stirring for a few minutes before adding 290 μL of TEOS. Finally, the resulting gel was stirred overnight at room temperature and then hydrothermally treated at 150 °C in a stainless steel Teflon-lined autoclave, under static conditions for 48 h. The solid obtained was washed thoroughly with water and dried at room temperature under vacuum. The calcinations of these materials were carried out in a nitrogen flow for 4 h at 550 °C and then switch to oxygen for 8 h more.

2.4. Characterization

UV–Vis spectra were obtained using an Agilent 8453 UV–Vis spectrophotometer (0.1 nm resolution). The as-synthesized samples were diluted (0.4 mL of fresh Pd nanoparticles, in toluene or water, were diluted to 10 mL with toluene or water, respectively) previously to their analysis. Transmission electron microscopy (TEM) studies were carried out on a JEOL JEM-2010 instrument. Several drops of the Pd sols were placed on a grid and the toluene evaporated at room temperature. In the case the Pd-nanoparticles-containing silica, the solid was suspended in methanol, sonicated and a few drops placed over the grid like previously described. For very small Pd nanoparticles, a Lacey Formvar/Carbon copper grid was used to reduce noise from the film grid. The digital analysis of the TEM Micrographs and particle size determination was done using DigitalMicrograph™ 3.6.1. by Gatan. Porous texture was characterized by N_2 adsorption at 77 and 273 K in an AUTOSORB-6 apparatus. The samples were previously degassed for 4 h at 523 K at 5×10^{-5} bars. The materials were also characterized by X-ray powder diffraction (SEIFERT 2002) using a CuKα (1.5418 Å) radiation at a scanning velocity of 0.02°/min in the $1° < 2\Theta < 8°$ range.

3. Results and discussion

3.1. Controlling Pd nanoparticles size

A preliminary study to produce Pd nanoparticles with controlled size and narrow pore size distribution was systematically carried out. The method developed by Brust et al. [44] was modified by increasing the concentrations of both the capping and reducing agent from 25 to 100 mmol/L, and from 0.1 to 1.2 mol/L, respectively. Whereas, no differences were found by changing the reducing agent concentration, the particle size decreased and particle size distribution narrowed from 1.66 ± 0.50 to 1.22 ± 0.15 nm when the capping agent concentration was increased from 25 to 50 mmol/L (see Table 1). However, higher concentrations namely, 100 mmol/L, did not produce any further change probably because the capping agent concentration was already too high. To better understand the influence of the water content in the Pd toluene colloidal suspension during nanoparticle formation, controlled amounts of water were added. As shown in Table 1, this parameter did not have a significant impact in the quality of the nanoparticles obtained. However, a further reduction of the particle size was obtained by increasing the stirring rate of the mixing reaction during the reduction of $[PdCl_4]^{2-}$. Nanosized particles with narrow particle size distribution, 1.03 ± 0.27 nm, were obtained when the reduction step was carried out at 1600 rpm.

Based on these results, the key synthesis parameters to obtain small nanoparticles with a narrow particle size distribution are the concentration of the capping agent and the stirring rate used during the reduction of the Pd precursor in toluene. In the first case, a certain concentration of tetraoctylammonium is required to efficiently cover the surface of the Pd nanoparticles, and in the second, a fast stirring rate produces the best results, probably due to the microemulsion formed with the aqueous droplets containing the reducing agent in the toluene phase where the $[PdCl_4]^{2-}$ is solved. A representative micrograph of this material, Pd32 as named in Table 1, is shown in Fig. 1. The XRD pattern of these Pd nanoparticles (not shown here) shows three distinctive low intensity peaks at 39.95, 46.80 and 67.9 2 θ (°), which correspond to the reflections due to the (111), (200) and (220) planes, respectively. This can be indexed as a face-centered cubic structure. The average particle size, obtained using the Scherrer equation, is 1.97 nm, in good agreement with the value obtained by TEM analysis.

3.2. Functionalized Pd nanoparticles as metallic replicas of surfactant micelles

Once high quality Pd nanoparticles were successfully prepared, the next step was to transfer these nanoparticles from the toluene to the water phase in order to be able to incorporate them in silica *via* sol–gel synthesis. This objective was successfully achieved by using DMAP as a transfer agent. This molecule has a neutral/zwitterion equilibrium. DMAP replaces the capping agent in the toluene phase, where it is in its neutral form, and quantitatively transfers the Pd nanoparticles to the water phase, where is present as a charged (zwitterion) species [45] (see Fig. 2).

The nanoparticles phase transfer has been corroborated using UV–Vis spectroscopy. As shown in Fig. 3, the colored phase due to the presence of Pd nanoparticles, initially the toluene (upper phase), is, after stirring, the water phase (bottom phase). Although colloidal dispersions of noble metals are known to display bright colors arising from surface plasmon resonances (SPR), in the case of Pd the dielectric function determines a resonance close to the UV, which overlaps with interband transitions. For this reason, the UV–Vis absorbance profile shown by the Pd nanoparticle toluene suspension does not show any surface plasmon band (Fig. 3, continuous line). On the contrary, the UV–Vis spectrum of Pd nanoparticle water suspension shows a clear absorption centered at 307 nm (Fig. 3, dotted line).

Pd nanoparticles can be prepared in organic phase at high contents with a small and homogeneous particle [45]. In our case, 1.2 g Pd/L toluene stable organosols were obtained using the

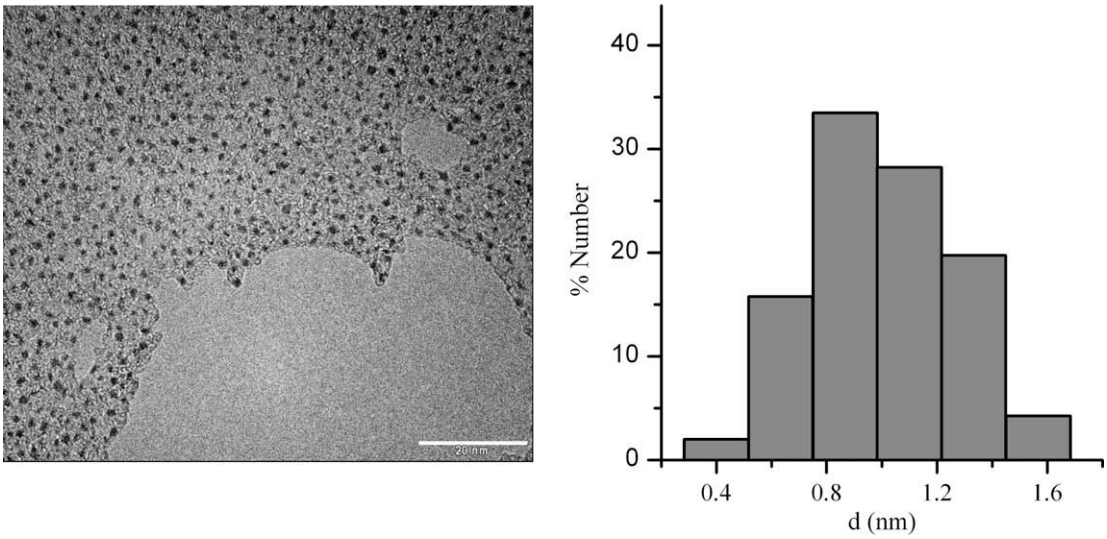

Fig. 1. Transmission electron microscopy (TEM) micrograph of Pd nanoparticles prepared by reduction of $[PdCl_4]^{2-}$ with $NaBH_4$ in toluene while stirring at 1600 rpm. The scale bar represents 20 nm.

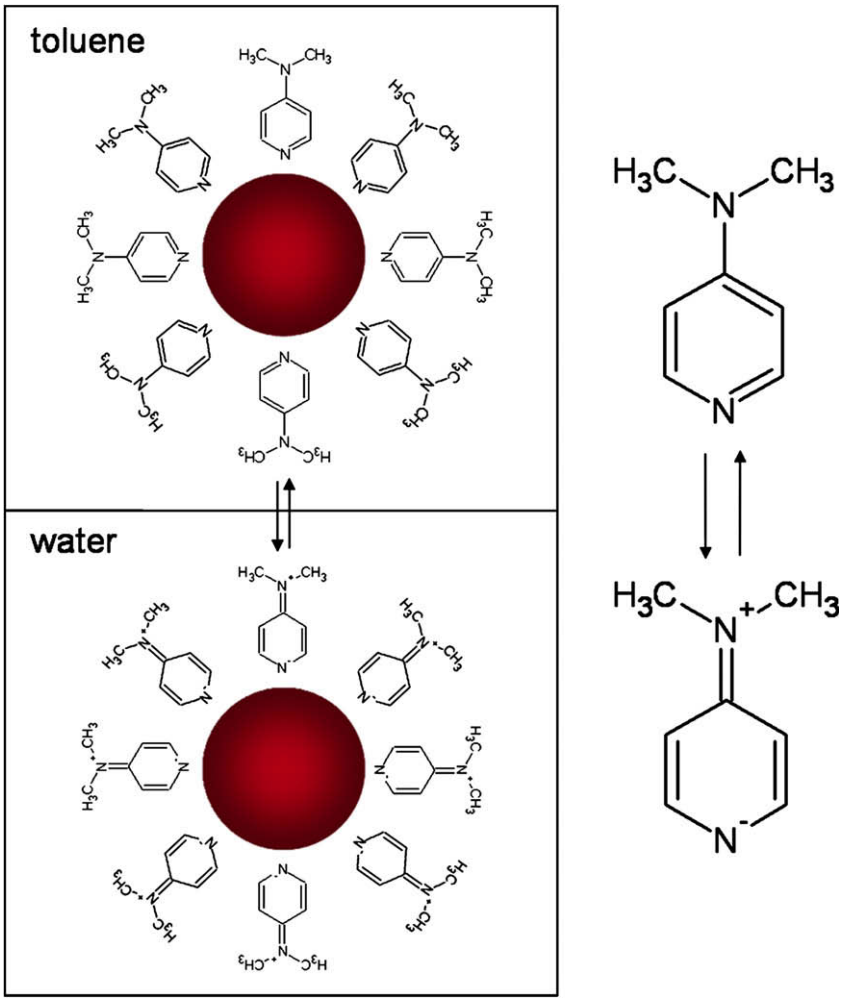

Fig. 2. Scheme of the experimental procedure used to transfer the Pd nanoparticles prepared in toluene to the aqueous phase. The transfer agent, dimethylaminopyridine (DMAP), neutral in the organic phase, is able to quantitatively extract the nanoparticles to the aqueous phase, where it is present as its zwitterion form. Adapted from Ref. [45].

conditions described in Section 2. Interestingly, the use of DMAP as transfer agent, also enables to further concentrate the suspension by liquid–liquid extraction into a smaller (until 4 times) volume of water without significant particle agglomeration (4.8 g Pd/L water).

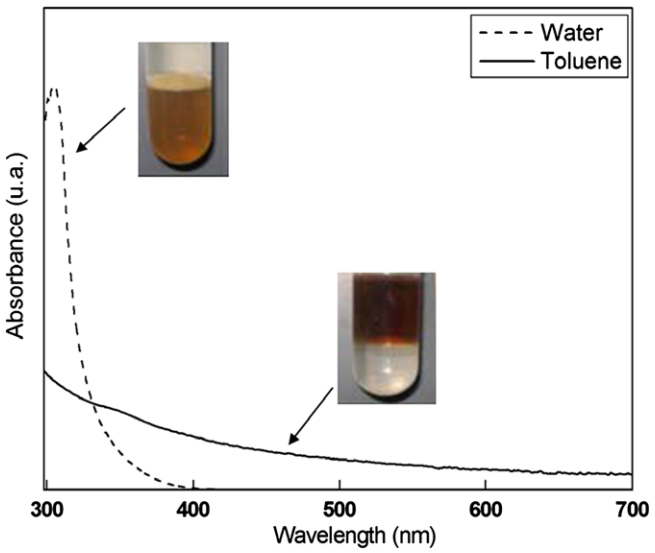

Fig. 3. Optical absorption spectra of Pd/tetraocthylammonium nanoparticles in toluene (continuous line) and aqueous Pd/DMAP nanoparticles (dotted line). The insets display the corresponding test tubes containing Pd nanoparticles before and after phase transfer.

In addition to serve as a transfer agent, DMAP functionalized on the surface of the Pd nanoparticles acting as a sort of metallic replica of a cationic surfactant micelle, with a metallic – instead of an alkyl – core, and a quaternary amine hydrophilic head. These functionalized nanoparticles were used as spherical templates to assemble silica around them by an M^+I^- mechanism similar to the S^+I^- used for the preparation of MCM-41 materials. The basic catalyzed hydrolysis of TEOS, which produces anionic silicates intermediates, in the presence of positively charged DMAP-functionalized Pd nanoparticles, produces an amorphous silica material with a homogeneous distribution of isolated Pd nanoparticles (Fig. 4b). This simple and effective nanoparticles loading method allows for a highly dispersed incorporation of the metal nanoparticles in silica. Compared to the more conventional impregnation method, it produces a higher metal dispersion allowing for high metal contents and the loading is not limited to the external surface of the support. Because silica was grown are the metal nanoparticles, their migration, agglomeration and leaching are notably prevented.

Compared to CVD, both the metal nanoparticle precursor and the preparation method are much simpler. Finally, metal loading by ion-exchange and subsequent reduction, is limited to materials with ion-exchange properties, mainly zeolites. The proposed method does not require successive ion exchange cycles and does not produce metal migration to the external surface and agglomeration during reduction. Compared to other incorporation methods, like the one recently described by Alvaro et al. [41], the one herein proposed is significantly simpler, does not require the preparation of costly silica precursors covalently bonded both to the nanoparticles and the surfactant molecule and allows for high contents of high quality nanoparticles.

An interesting observation is the size-selective incorporation of Pd nanoparticles in the silica matrix. Even if one starts from a suspension containing both small and large nanoparticles (Fig. 4a), the final solid only contains the small particles since these are readily embedded whereas the bulkiest ones are excluded of the silica matrix (Fig. 4b).

3.3. Incorporation of Pd nanoparticles in mesostructured silica

As aforementioned, the next step in this synthesis strategy is the incorporation of metal nanoparticles in mesostructured silica, so they can be accessible to reactants and therefore being used for catalysis, sensing and further chemical modification. Two different methods have been developed to achieve this goal:

(i) The combined use of DMAP-functionalized Pd nanoparticles and CTAB, used as MCM-41 templates. The cationic shell of both supramolecular templates produces a homogenous incorporation of both metal nanoparticles and mesoporosity, allowing for the direct and facile preparation of MCM-41 with Pd nanoparticles embedded in its mesopore walls. Especially remarkable is the very high Pd content (over 60 wt.% Pd in silica) that can be archived using this strategy.

(ii) The functionalization of Pd nanoparticles with mercaptopropyltriethoxysilane (MPTES) and subsequent co-polymerization with TEOS by basic catalyzed hydrolysis, used

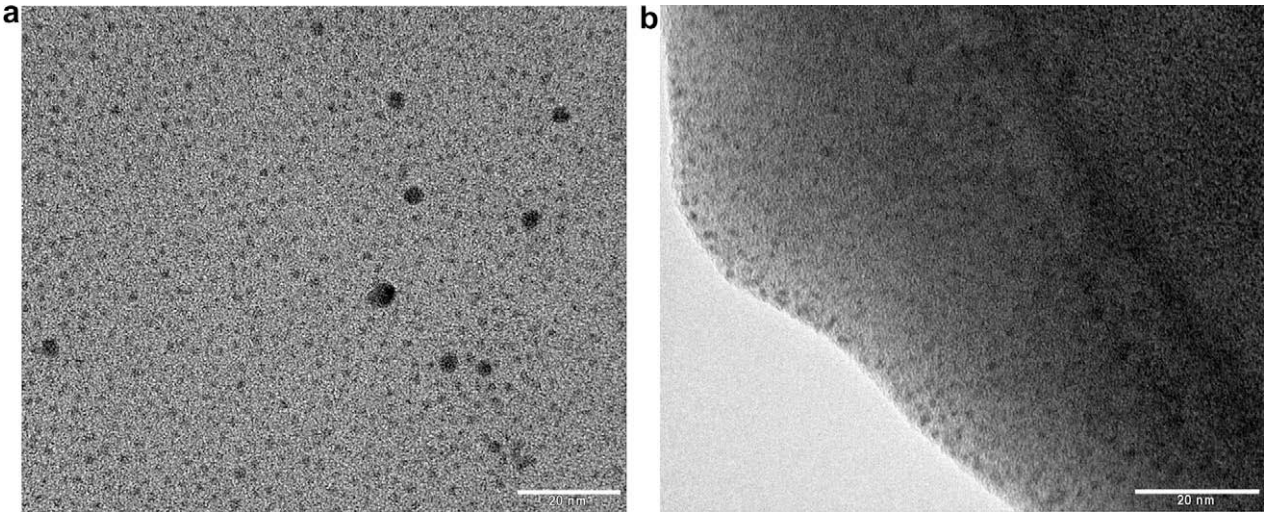

Fig. 4. TEM micrographs of Pd nanoparticles before and after being incorporated in amorphous silica by base-catalyzed hydrolysis of TEOS in an aqueous DMAP-functionalized Pd nanoparticles sol. (a) Special preparation in which small (1–2 nm) and large (3–5 nm) nanoparticles are observed before Pd nanoparticles incorporation in silica. (b) Pd nanoparticles incorporated in amorphous silica. Only small (1–2 nm) nanoparticles are observed once selectively incorporated in the silica matrix. The scale bar represents 20 nm.

as silica precursors. The idea behind this second method is inspired on the use of bridged organosilanes precursors ($((CH_3(CH_2)_nO)_3Si\text{-}R\text{-}Si(O((CH_2)_nCH_3)_3)$) to smartly and homogenously introduce different functionalities in mesostructured silicas (see Fig. 5a). In this case, the use of metallosilanes precursors (metal nanoparticles covalently bonded to trialkoxysilane terminal groups) also allows for the homogeneous in-situ incorporation of metal nanoparticles covalently bonded to the porous support. Some flexibility has been allowed by the use of a spacer (the propyl group) between the thiol group (responsible of the covalent bond with the nanoparticles) and the three silane groups. The addition of CTAB to the synthesis solution allows also for the production of MCM-41 with Pd nanoparticles embedded in its mesopore walls.

Interestingly, the direct incorporation of MPTES-functionalized Pd nanoparticles in a silica matrix was not possible without the assistance of CTAB since no significant silica formation was observed in its absence. Under the experimental conditions used, this cationic surfactant is needed to induce the precipitation of the silica by electrostatic interaction as described in the S^+I^- mechanism. Only in the case of DMAP-functionalized nanoparticles (which have a positively charged shell) the precipitation of the silica occurs without the assistance of CTAB. The M^+I^- suggested in this case is likely to be responsible of the size-selective incorporation of the metal nanoparticle in the silica matrix, since some sizes will more efficiently compensate the negative charge of the silica soluble intermediate species.

3.3.1. Combined use of DMAP-functionalized Pd nanoparticles and CTAB to produced MCM-41 with Pd nanoparticles in its walls

Key synthesis parameters were systematically modified to optimize the incorporation of DMAP-functionalized Pd nanoparticles in MCM-41 (Table 2). Fig. 6 shows the XRD pattern (bottom) of the calcined materials prepared using this synthesis strategy. This pattern has a distinctive broad peak at low angle which is characteristic of mesostructured material. The lack of other peaks does not allow a more specific structure determination. The mesoporous nature of the calcined materials was confirmed by nitrogen adsorption at 77 K. Its type IV isotherm (see Fig. 7a, bottom) displays a sharp uptake at 0.3–0.4 P/P_0, and no hysteresis loop. As shown in Fig. 7b, these materials, with a BET surface of 495 m^2/g, show a bimodal pore size distribution with two peaks centered at 2.5 and 4.0 nm.

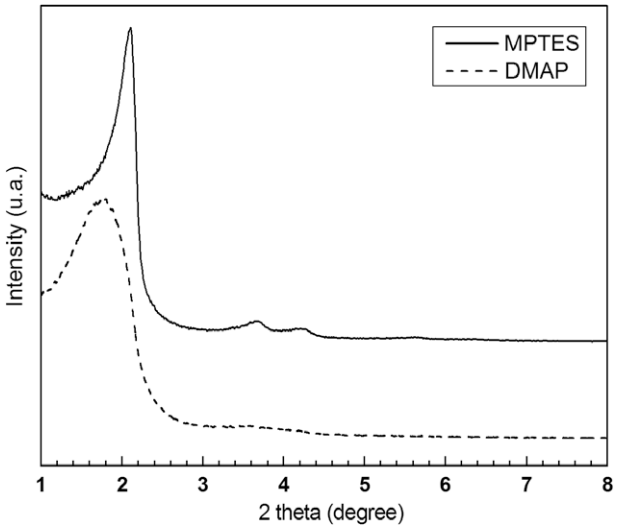

Fig. 6. X-ray diffraction patterns of a sample prepared by hydrolysis of TEOS in the presence of CTAB and triethoxysilane-functionalized Pd nanoparticles (top) and DMAP-functionalized Pd nanoparticles (bottom).

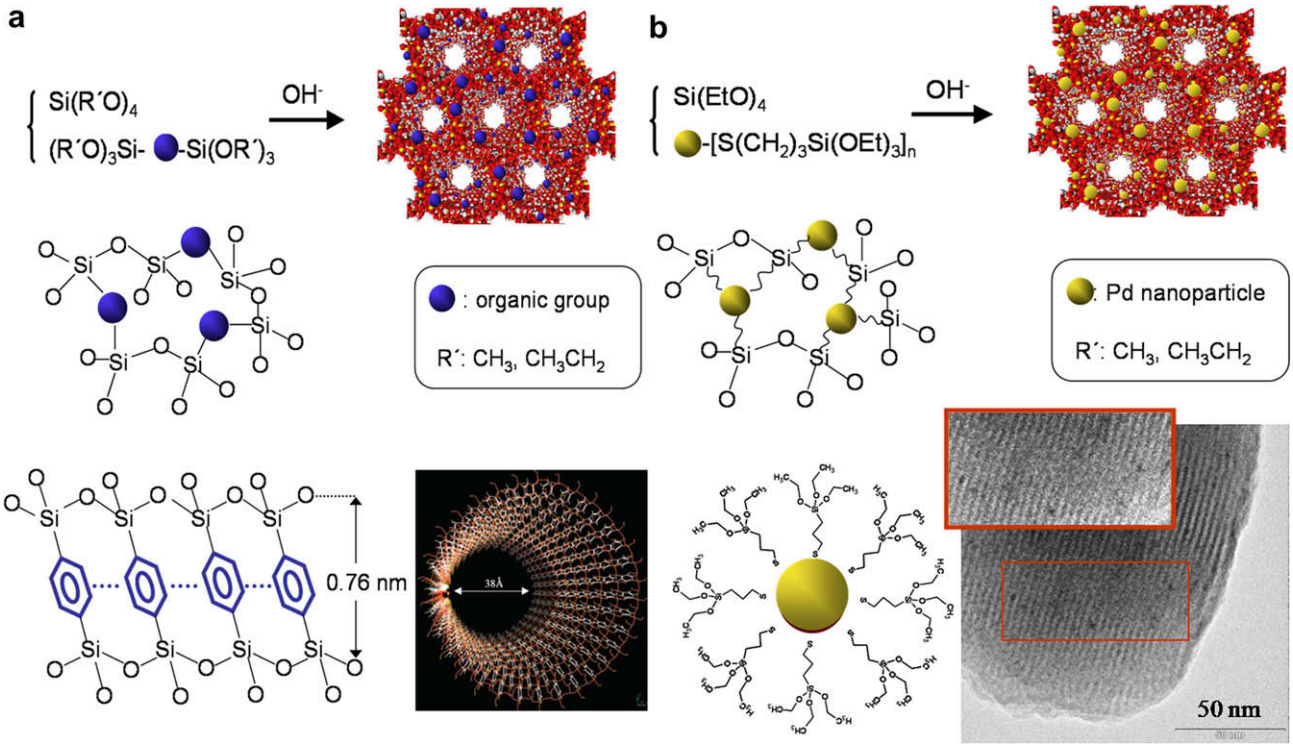

Fig. 5. Schematic of the incorporation of different entities in the pore walls of mesoporous silica. (a) Incorporation of organic groups using bridged organosilane precursors (top) and schematic of the structure of a phenylene-bridged hybrid mesoporous organosilica with both atomic and mesoporous periodicity (bottom). (b) Incorporation of metal nanoparticles using trialkoxysilane-functionalized nanoparticles (top) and TEM micrograph of Pd nanoparticles incorporated in periodic mesoporous silica (bottom).

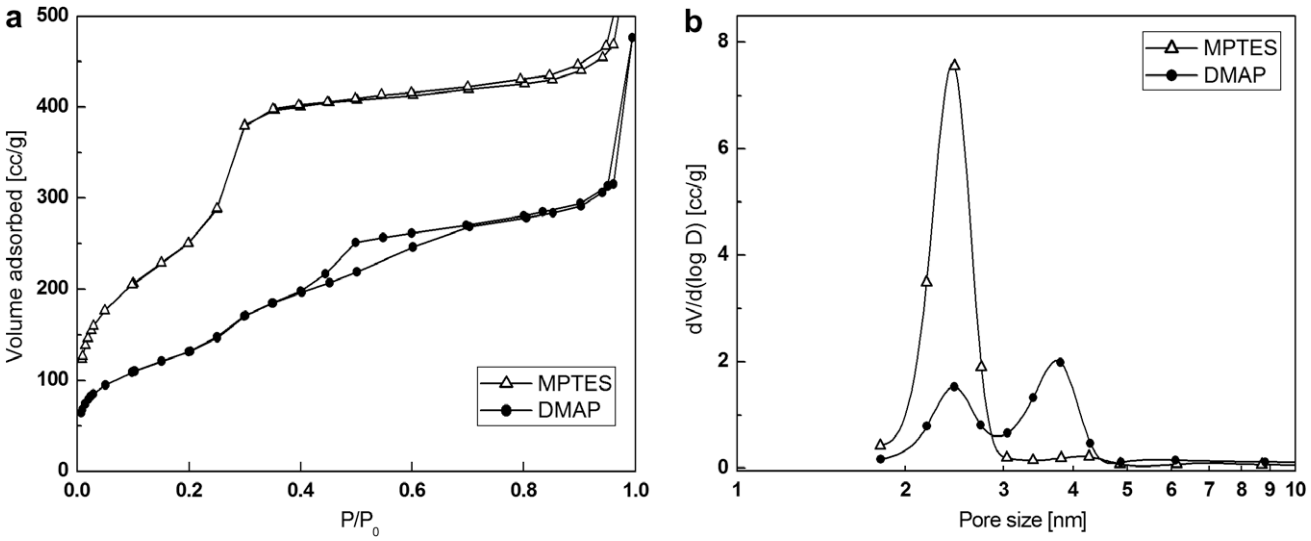

Fig. 7. (a) Nitrogen adsorption/desorption isotherms at 77 K and (b) corresponding pore size distribution (BJH method) of a sample prepared by hydrolysis of TEOS in the presence of CTAB and triethoxysilane-functionalized Pd nanoparticles (top, triangles) or DMAP-funtionalized Pd nanoparticles (bottom, circles).

Interestingly, the calcination step carried out to remove the surfactant does not significantly increase nanoparticle size, as observed by TEM (not shown here). This result supports our initial assumption that embedded (incorporated) nanoparticles agglomerate less than impregnated nanoparticles, probably due to the restricted mobility.

3.3.2. Trialkoxysilane-functionalized nanoparticles as metallosilica precursors for smart metal incorporation in mesostructured silica

Fig. 6 presents the XRD patterns of both the MCM-41 containing DMAP-functionalized Pd nanoparticles (bottom) and the MCM-41 containing trialkoxysilane-functionalized Pd nanoparticles (top). Only the latter presents several well-defined peaks, which indicates a more ordered mesoporosity and therefore a higher quality MCM-41, also confirmed by nitrogen adsorption at 77 K (see Fig. 7a). Its corresponding pore size distribution displays only one well-defined peak centered at 2.5 nm (Fig. 7b). This pore size is also observed for the material prepared with DMAP-functionalized Pd nanoparticles. This observation suggests that this mesoporosity is due to the templating effect of CTAB.

The higher BET surface, 921 m^2/g, the unimodal size distribution (see Fig. 7b), and the well-defined XRD pattern (Fig. 6, continuous line) of the materials prepared using Pd nanoparticles functionalized with trialkoxysilanes evidence that this strategy produces more ordered MCM-41 than DMAP-functionalized Pd nanoparticles. It is likely that the quaternary ammine-functionalized Pd nanoparticles interfere with the self-assembly of the CTAB micelles, producing a bimodal less ordered mesoporous material.

Transmission electron microscopy has also been used in this case to confirm both the quality of the MCM-41 mesostructure and the high dispersion of isolated Pd nanoparticles homogeneously distributed throughout the silica material. Fig. 8 shows representative TEM micrographs before (a) and after calcination (b) for MCM-41 containing trialkoxysilane-functionalized Pd nanoparticles. It has been not possible to distinguish the very small Pd nanoparticles in the uncalcined material, although their presence has been confirmed by X-ray microanalysis (TEM–EDX). Noteworthy, the size of the nanoparticles remain very small (below 2 nm) even after heat treatment at 550 °C for 8 h. The calcination does not produce any significant migration of the nanoparticles which

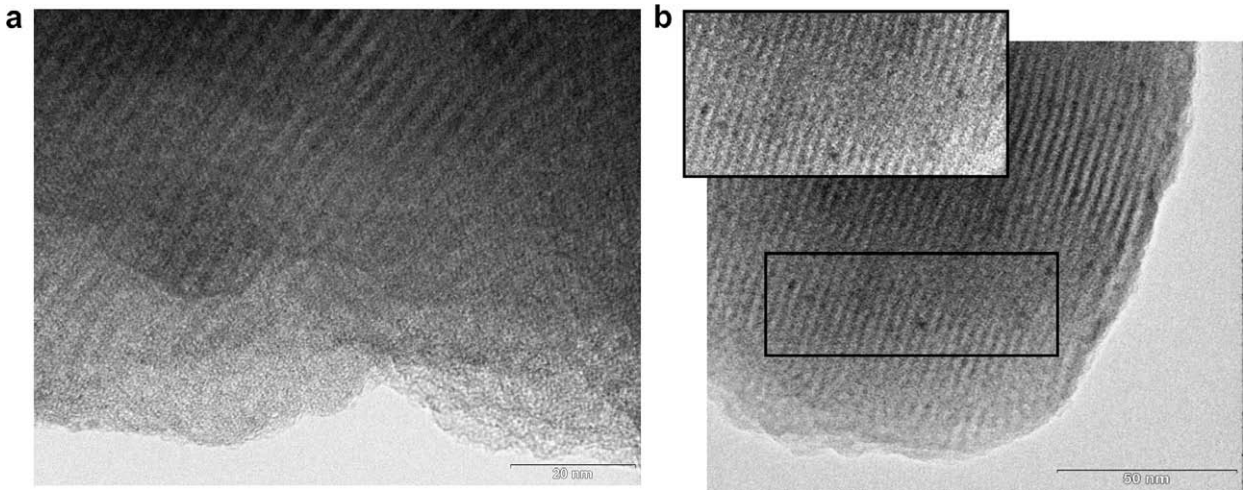

Fig. 8. Representative TEM micrographs of Pd nanoparticles incorporated in MCM-41 using triethoxysilane-functionalized Pd nanoparticles (a) before and (b) after calcinations. The scale bars represent 20 and 50 nm, respectively.

can be distinguished inside the straight mesoporosity of the support.

4. Conclusions

Two different strategies have been developed to obtain highly dispersed Pd nanoparticles incorporated in silica matrices. These methods are based on the use of functionalized metal nanoparticles as (i) metallic replicas of surfactant micelles and as (ii) building blocks for the construction of silica materials.

Mimicking cationic surfactant micelles, metallic replicas were prepared by functionalizing Pd nanoparticles with quaternary amines. The base-catalyzed hydrolysis of alkoxysilanes in the presence of these positively charged metal nanoparticles, induces the precipitation of the silica around the cationic templates by a electrostatic M^+I^- mechanism. The addition of CTAB to the synthesis solution produces controlled mesoporosity. This method allows for easy, direct and highly homogeneous metal nanoparticle incorporation in mesoporous solids.

Recently, other groups have prepared the so-called organosilicas by condensation of organic-containing silica precursors (trialkoxysilane-R-trialkoxysilane, being R an organic group) with the tetraalkoxysilanes. Inspired on this strategy, nanoparticle-containing mesoporous silicas were prepared by condensation of metal nanoparticles covalently bonded to trialkoxysilane terminal groups with tetraalkoxysilanes in the presence of CTAB. Both the surfactant and the functional groups can be removed by calcination, producing a material with Pd nanoparticle homogeneously and highly dispersed in a mesoporous support. The cavity, in which the metal nanoparticle is located after the functional groups are removed, inhibits the migration of the nanoparticle and thus the agglomeration/sintering. These methods are general and should also serve to incorporate other metal nanoparticles and other types of nanoparticles (like metal oxides) in silica matrices.

Acknowledgments

This research has been funded by the Ministerio de Educación y Ciencia (CTQ2005-09385-C03-02). J.G.M. and A.R. are grateful for financial support under the Ramón y Cajal program. Cristina Almansa Carrascosa is kindly thanked for assistance with Transmission Electron Microscopy.

References

[1] E. Roduner (Ed.), Nanoscopic Materials Size-Dependent Phenomena, RSC Publishing, Cambridge, 2006. pp. 239–262.
[2] C.N.R. Rao, A. Müller, A.K. Cheetham (Eds.), The Chemistry of Nanomaterials, Wiley-VCH, Weinheim, 2004.
[3] G. Ozin, A. Arsenault (Eds.), Nanochemistry: A Chemical Approach to Nanomaterials, RSC Publishing, Cambridge, 2005.
[4] C. Solans, P. Izquierdo, J. Nolla, N. Azemar, M.J. Garcia-Celma, Curr. Opin. Colloid Interface Sci. 10 (2005) 102.
[5] P.-F. Ho, K.-M. Chi, Nanotechnology 15 (2004) 1059.
[6] C.T. Kresge, M.E. Leonowicz, W.J. Roth, J.C. Vartuli, J.S. Beck, Nature 359 (1992) 710.
[7] A. Corma, A. Martínez, V. Martínez-Soria, J.B. Monton, J. Catal. 153 (1995) 25.
[8] U. Junges, W. Jacobs, I. Voigt-Martín, B. Krutzsch, F. Schüth, J. Chem. Soc., Chem. Commun. (1995) 2283.
[9] D. Brunel, Micropor. Mesopor. Mater. 27 (1999) 329.
[10] M.J. Verhoef, P.J. Kooyman, J.A. Peters, H. van Bekkum, Micropor. Mesopor. Mater. 27 (1999) 365.
[11] W. van Rhijn, D. De Vos, W. Bossaert, J. Bullen, B. Wouters, P. Grobet, P.A. Jacobs, Stud. Surf. Sci. Catal. 117 (1998) 183.
[12] K.R. Kloetstra, H. van Bekkum, J. Chem. Soc., Chem. Commun. (1995) 1005.
[13] K.R. Kloetstra, M. van Laren, H. van Bekkum, J. Chem. Soc., Faraday Trans. 93 (1997) 1211.
[14] X.H. Lin, G.K. Chuah, S. Jaenicke, J. Mol. Catal. A: Chem. 190 (2000) 43.
[15] C.A. Koh, R. Nooney, S. Tahir, Catal. Lett. 47 (1997) 199.
[16] S.I. Cho, D.S. Kim, S.I. Woo, Korean J. Chem. Eng. 14 (1997) 479.
[17] R.Q. Long, R.T. Yang, Catal. Lett. 52 (1998) 91.
[18] B.S. Uphade, M. Okumura, S. Tsubota, M. Haruta, Appl. Catal. A: Gen. 190 (2000) 43.
[19] U. Junges, F. Schüth, G. Schmid, Y. Uchida, R. Schlögl, Ber. Bunsenges, Phys. Chem. 101 (1997) 1561.
[20] T. Abe, Y. Tachibana, T. Uematsu, M. Iwamoto, J. Chem. Soc., Chem. Commun. (1995) 1617.
[21] M. Fröba, R. Kohn, G. Bouffard, O. Richard, G. van Tendeloo, Chem. Mater. 11 (1999) 2858.
[22] E. Barea, X. Batlle, P. Bourges, A. Corma, V. Fornes, A. Labarta, V.F. Puntes, J. Am. Chem. Soc. 127 (2005) 18026.
[23] E.M. Barea, V. Fornes, A. Corma, P. Bourges, E. Guillon, V.F. Puntes, Chem. Commun. (2004) 1974.
[24] Y. Wu, L. Zhang, G. Li, C. Liang, X. Huang, Y. Zhang, G. Song, J. Jia, C. Zhixiang, Mater. Res. Bull. 36 (2001) 253.
[25] T.J. Krinke, K. Deppert, M.H. Magnusson, H. Fissan, Part. Part. Syst. Char. 19 (2002) 321.
[26] H. Hofmeister, P.T. Miclea, W. Mörke, Part. Part. Syst. Char. 19 (2002) 359.
[27] W.-H. Zhang, J.-L. Shi, L.-Z. Wang, D.S. Yan, Chem. Mater. 12 (2000) 1408.
[28] M. Hartmann, S. Racouchot, C. Bischof, Micropor. Mesopor. Mater. 27 (1999) 309.
[29] R. Köhn, M. Fröba, Catal. Today 68 (2001) 227.
[30] L. Zhang, J. Shi, J. Yu, Z. Hua, X. Zhao, M. Ruan, Adv. Mater. 14 (2002) 1510.
[31] H. Winkler, A. Birkner, V. Hagen, I. Wolf, R. Schmechel, H. Seggern, R.A. Fischer, Adv. Mater. 11 (1999) 1444.
[32] C. Yang, P. Liu, Y. Ho, C. Chiu, K. Chao, Chem. Mater. 15 (2003) 275.
[33] Z. Kónya, V.F. Punters, I. Kiricsi, J. Zhu, J.W. Ager III, M.K. Ko, H. Frei, P. Alivisatos, G.A. Somorjai, Chem. Mater. 15 (2003) 1242.
[34] Z. Zhang, S. Dai, X. Fan, D.A. Blom, S.J. Pennycook, Y. Wei, J. Phys. Chem. B 105 (2001) 6755.
[35] A. Fukuoka, H. Araki, Y. Sakamoto, N. Sugimoto, H. Tsukada, Y. Kumai, Y. Akimoto, M. Ichikawa, Nano Lett. 2 (2002) 793.
[36] A. Fukuoka, H. Araki, J. Kimura, Y. Sakamoto, T. Higuchi, N. Sugimoto, S. Inagaki, M. Ichikawa, J. Mater. Chem. 14 (2004) 752.
[37] Y. Plyuto, J.M. Berquier, C. Jacquiod, C. Ricolleau, Chem. Commun. (1999) 1653.
[38] S. Besson, T. Gacoin, C. Ricolleau, J.P. Boilot, Chem. Commun. (2003) 360.
[39] S. Chytil, W.R. Glomm, E. Vollebekk, H. Bergem, J. Walmsley, J. Sjöblom, E.A. Blekkan, Micropor. Mesopor. Mater. 86 (2005) 198.
[40] C. Aprile, A. Abad, H. García, A. Corma, J. Mater. Chem. 15 (2005) 4408.
[41] M. Alvaro, C. Aprile, H. García, C.J. Gómez-García, Adv. Funct. Mater. 16 (2006) 1543.
[42] G. Budroni, A. Corma, Angew. Chem. Int. Ed. 45 (2006) 3328.
[43] G. Budroni, A. Corma, H. García, A. Primo, J. Catal. 251 (2007) 345.
[44] M. Brust, M. Walker, D. Bethell, D.J. Schiffrin, R. Whyman, J. Chem. Soc., Chem. Commun. (1994) 801.
[45] D.I. Gittins, F. Caruso, Angew. Chem. Int. Ed. 40 (2001) 3001.
[46] A. Berenguer-Murcia, J. García-Martínez, D. Cazorla-Amorós, A. Martínez-Alonso, J.M. Díez-Tascón, A. Linares-Solano, Stud. Surf. Sci. Catal. 144 (2003) 83.